

Reversible Data Hiding in Encrypted Images Using MSBs Integration and Histogram Modification

Ammar Mohammadi, Mohammad Ali Akhaey and Mansor Nakhkash

Abstract— This paper presents a reversible data hiding in encrypted image that employs based notions of the RDH in plain-image schemes including histogram modification and prediction-error computation. In the proposed method, original image may be encrypted by desire encryption algorithm. Most significant bit (MSB) of encrypted pixels are integrated to vacate room for embedding data bits. Integrated ones will be more resistant against failure of reconstruction if they are modified for embedding data bits. At the recipient, we employ chess-board predictor for lossless reconstruction of the original image by the aim of prediction-error analysis. Comparing to existent RDHEI algorithms, not only we propose a separable method to extract data bits, but also content-owner may attain a perfect reconstruction of the original image without having data hider key. Experimental results confirm that the proposed algorithm outperforms state of the art ones.

Index Terms—Histogram modification, prediction-errors, reversible data hiding, vacating room after encryption.

I. INTRODUCTION

Reversible data hiding in plain-image (RDHPI) is drastically developed by many researchers in recent years [1]. In RDHPI secret data imperceptibly is embedded in a plain-image in a way that original image can be losslessly recovered after secret data extraction. More presented papers in RDHPI drive from three main notions that are difference expansion, histogram modification and lossless compression respectively pioneered by [2], [3] and [4]. More developed papers also employ prediction-error to improve hiding capacity in a determined level of distortion. Whatever more accurate prediction is attained, there is sharper histogram of the errors that can be modified to embed secret data. For example, schemes in [5] and [6] exploit gradient-adjusted prediction (GAP) and median edge detector (MED) predictors that firstly are introduced in [7] and [8], respectively. Tsai et al. [9] present a predictor, may be denoted local difference (LD) predictor, that computes difference between pixels intensities in a local area of the image and most central one in the area to bring out prediction-errors. They embed secret data via histogram modification of the prediction-errors. Sachnev et al. further present cross-dot predictor that divides image into two “cross” and “dot” sets [10]. Dot set may be predicted using cross one and vice versa. Cross-dot predictor is also represented as chessboard (CB) predictor in [11].

Besides RDHPI, reversible data hiding in encrypted image (RDHEI) is a new need of cloud computing attracted intensive attention of the researchers. In RDHEI there are three parties: image-owner, data hider and recipient. Image-owner may not trust a channel administrator (or inferior assistant) so the image-

owner encrypts the image before uploading to cloud server while image-owner is not motivated to compress original-content before encryption. On the other side, data hider, i.e. the channel administrator, is not allowed to have original-content but authorized to embed some handy data in the encrypted image. The approach should guarantee lossless original image reconstruction and error-free data extraction at the recipient. These challenges are the cause of developing RDHEI.

Schemes introduced in RDHEI may be classified into three categories, namely reserving room before encryption (RRBE) [12-19], vacating room by encryption (VRBE) [20-26] and vacating room after encryption (VRAE) [27-32].

In RRBE there is a pre-processing before encryption that enables data hider to embed data bits in the encrypted image.

Most notions in VRBE are realized by encrypting some pixels intensities in a local area of the image using same cipher bytes. The approach preserves correlation between pixels employed to embed data bits. Thus, some information remains disclosed in VRBE.

The schemes presented in RRBE and VRBE are separable means extraction of the data bits at the recipient are not tied to decrypted information. On the other hand, in joint ones data extraction can be attained just using decrypted marked image.

In VRAE procedure, data hider is completely blind to original information. After image encryption, data hider vacates rooms to embed data bits without any knowledge of original-content. Some methods in VRAE are joint [28, 30, 31] and some others are separable [27, 29]. In [32], two different joint and separable procedure are introduced. The separable schemes in VRAE are more functional than joint ones and also RRBE and VRBE. Since they are absolutely blind to original-content, they preserve content-owner privacy more than others. However, achieving high embedding capacity is more challengeable in separable VRAE than others.

On the security term in using secret keys, Chen et al. [15] classify three different schemes: namely share independent secret keys (SIK), shared one key (SOK) [15] and share no secret keys (SNK) [12, 17]. In SIK there exist two data hider (K_d) and image-owner (K_e) keys that are shared with recipient independently while in SOK there exists just one key and in SNK there exists no key to be shared. Most schemes in RDHEI, including presented VRBE and VRAE schemes, employ SIK to manage secret keys.

In general kind of view, similar to RDHPI, most schemes in RDHEI employ correlation of neighboring pixels in an image and further they employ based idea or procedure of RDHPI such as histogram modification, difference expansion and

prediction-error computation. As an example, schemes [15, 17] exploit difference expansion and further, scheme [12] employs histogram modification of the prediction-errors to reserve room before encryption. Huang et al. present new framework in RDHEI that makes possible using most notions of RDH in plain-image for encrypted one [24]. In this self-contained scheme any kind of prediction technique, including GAP, MED, CB and LD may be used to bring out prediction-errors.

Schemes [19] and [20] use idea of LD predictor to embed data in the encrypted image. They realize lossless reconstruction (LR) of the original image and error-free extraction of data bits. Also, scheme [29] employs local correlation of neighboring pixels to reconstruct original one at the recipient. Using MED predictor, Yin et al. bring out some labels for almost all pixels before encryption [14]. These labels then are compressed via Huffman coding to be embedded along with data bits. They improve [19] and [20] naturally with the aim of source coding.

Fallahpour and Sedaaghi [33] present a RDHPI method that apply scheme [3] in non-overlapped blocks of the plain-image to embed data using histogram modification of pixels in a block. In the same approach, Ge et al. [25] introduce a RDHEI method that employs histogram modification ([3]) in non-overlapped blocks of the encrypted one to vacate room for embedding data bits.

As discussed, there are several schemes in RDHEI that employ based notions of RDHPI to embed data in the encrypted image. As well, we present a new scheme in RDHEI that uses based idea of the histogram modification to vacate room after encryption. Data bits just are embedded in MSBs of target pixels that are integrated to be prepared for histogram modification. Target pixels are the ones used for embedding data bits. As another notion that is employed in RDHPI methods, we use CB predictor for LR of the original image at the recipient. We use independent secret keys, k_c and k_d to encrypt original image and data bits, respectively.

In our scheme, not only data bits perfectly are extracted but also data extraction process is separated from original image reconstruction. Proposed scheme can be considered as a functional method that improves state of the art RDHEI schemes.

The rest of the paper is organized as follows. Related works are discussed in section II. The proposed method is presented in section III including both embedding and error-free extraction of data bits and lossless reconstruction of the original image. Section IV demonstrates the experimental results. Finally section V concludes the paper.

II. RELATED WORKS

Proposed method is inspired from histogram modification. Besides, we employ CB predictor to reconstruct original image at the recipient by analyzing prediction-error. They are discussed in more details in this section.

A. Histogram modification

As discussed, Ni et al. [3] present a RDHPI scheme using histogram modification of the original image. In the approach,

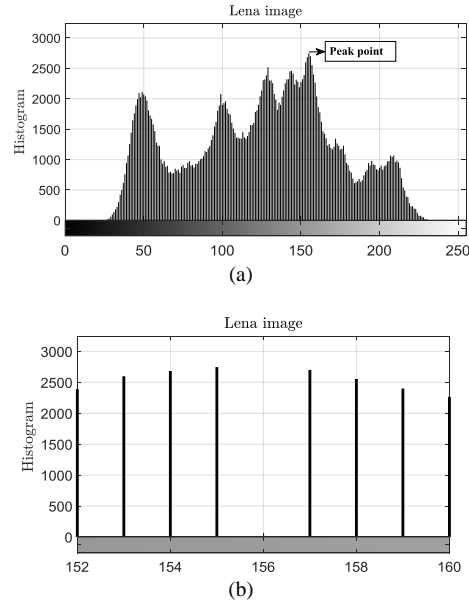


Fig. 1. (a) Histogram of Lena image. (b) Vacate room to embed data bits.

they embed data bits in peak point of the histogram that is a pixel with most frequent in the image. Accordingly, they vacate room by histogram modification (VRHM) to provide empty position used for embedding data. In the approach, reversible reconstructing of the original image is possible. For the example, peak point in the histogram of Lena (Fig. 1a) is “155”. One to vacate room adds all intensities of the image more than “155” by 1 (Fig. 1b) providing space to embed data bits.

In the proposed procedure, we apply the idea of VRHM in the encrypted image.

B. Chess-board predictor

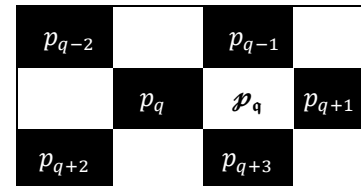


Fig. 2. Part of an image, whose pixels are divided into white and black sections.

The CB predictor, i.e. non-causal, can provide prediction better than MED and GAP, causal ones. As shown in Fig. 2, in CB predictor, a black/white pixel may be predicted using white/black neighbors. For example, prediction of a white pixel p_q employing neighboring black ones $\{p_{q-1}, p_q, p_{q+1}, p_{q+3}\}$ is done by

$$\tilde{p}_q = \lfloor \frac{p_{q-1} + p_q + p_{q+1} + p_{q+3}}{4} \rfloor \quad (1)$$

where $\lfloor . \rfloor$ is the round function. Using \tilde{p}_q and p_q , the prediction-error e_q is computed by

$$e_q = p_q - \tilde{p}_q \quad (2)$$

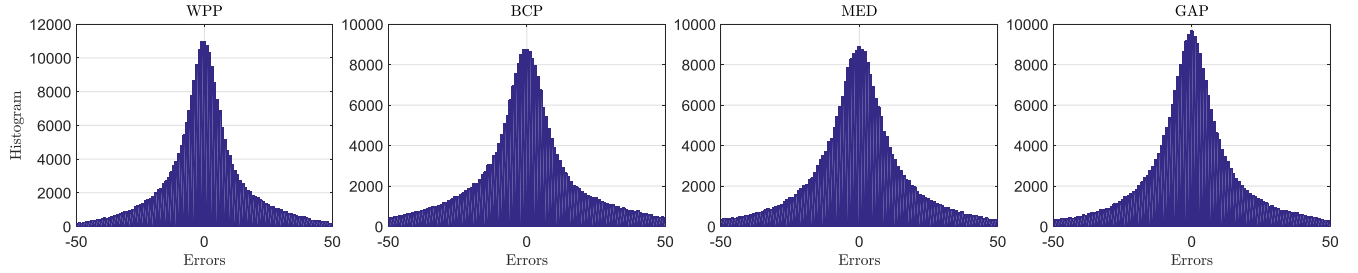


Fig. 3. Histograms of prediction-errors provided by MED, GAP, BCP and WPP predictors for Baboon image.

more specifically let's denote the prediction of a white pixel by neighboring black ones as white plus prediction (WPP). In addition, a central black pixel (P_q) can be predicted using neighboring black ones, $\{P_{q-2}, P_{q-1}, P_{q+2}, P_{q+3}\}$, by

$$\tilde{p}_q = \lfloor \frac{P_{q-2} + P_{q-1} + P_{q+2} + P_{q+3}}{4} \rfloor \quad (3)$$

that denoted black cross prediction (BCP). Similarly, in BCP, prediction-error is calculated by

$$e_q = p_q - \tilde{p}_q \quad (4)$$

C. Prediction-error analysis

According to (2) or (4), having a prediction-error and a predicted value of an original pixel, definitely, it can be reconstructed. However, in [19] we prove that even having a range of the prediction-error, reconstructing some significant bits of the original pixel still is possible. To be more clarified, let's assume a prediction-error (ϵ) that is computed subtracting the original pixel (p) and its predicted value (\tilde{p}).

$$p - \tilde{p} = \epsilon \quad (5)$$

In [19] we confirm that, particularly, a bit embedding capacity (EC) will be provided in MSB of the pixel “ p ” when the error satisfies

$$|\epsilon| < 64 \quad (6)$$

To gain a better insight, let's assume a pixel, $p = p_7p_6p_5p_4p_3p_2p_1p_0$, that describes eight bits including LSB, p_0 , to MSB, p_7 . Having (6), p_7 may be replaced by a data bit in a way can be retrieved at the recipient.

Employing more efficient predictor realizes sharper histogram of the prediction-errors and accordingly provides the more pixels in the image that their prediction-errors verify (6). Thus, there exist more MSBs of the pixels to be modified for embedding data bits.

In Fig. 3, histograms of prediction-errors provided by MED, GAP, BCP and WPP predictors are demonstrated for Baboon image. BCP and WPP predictors are applied for all pixels. As shown, WPP provides sensibly a sharper histogram of the prediction-errors than others. In addition, as seems GAP makes sharper histogram than MED and BCP. In meanwhile, the more important subject is answer to this question “how many do

prediction-errors exist which their absolute values are greater than 64 ?”. They can not be exploited to embed even one data bit because they do not verify (6). Let's denote “ l ” as the number of prediction-errors do not confirm (6) and “ L ” as the all prediction-errors in an image. Accordingly, we define

$$f_{predictor} = l/L \quad (7)$$

as a probability of failure in reconstruction of a reformed MSB of a pixel randomly picked up. Accordingly, we have $f_{WPP} = 0.0017$, $f_{BCP} = 0.021$, $f_{GAP} = 0.014$ and $f_{MED} = 0.016$ for Baboon image. Although f_{WPP} significantly is less than others, there still exists a probability of failure in reconstruction of the original pixels. As a solution, we combine several MSBs of the target pixels diminishing risk of failure. Therefore, N ones of the MSBs are integrated and so integrated one is used to carry data bit. It can be proved that there is always a N can be taken to guarantee LR of the original pixels.

The amount of computed $f_{pre.}$ depends not only on the kind of an employed predictor, but also the type of a host image. The lower the entropy may be provided by an image, the lower the probability of the failure can be attained in recovering. In other words, generally, smoother images have less $f_{pre.}$, e.g. unlike Baboon, Lena and F16 have $f_{WPP} = 0$.

Accordingly, in the proposed method we employ WPP predictor. We may also exploit BCP to improve EC.

III. PROPOSED SCHEME

In this section, we introduce the proposed method in details including image encryption, simple scrambling and unscrambling, embedding and extracting data bits, recovering the original image and overall view of the proposed method.

A. Image encryption

Encryption of the original image is done using content-owner secret key, K_e . However, for encryption, not only any method of encryption but also any standard encryption algorithm can be exploited. The only restriction is no change in positions of the image pixels during encryption. If it occurs, data hider will have knowledge of the new positions to realize proposed procedure. Therefore, in term of security, content-owner can chose a desire encryption algorithm.

Regarding O as the original image, encrypted image is denoted \hat{O} . Accordingly, let's classify pixels formed \hat{O} into two groups, namely encrypted white target pixels (EWTPs),

$\{\hat{p}_0, \hat{p}_1, \dots, \hat{p}_q, \dots, \hat{p}_Q\}$ and encrypted black pixels (EBPs), $\{\hat{p}_0, \hat{p}_1, \dots, \hat{p}_q, \dots, \hat{p}_Q\}$. Encrypted black pixels are also composed of encrypted black reference pixels (EBRPs) and encrypted black target pixels (EBTPs). EBRPs remain intact during data embedding process and are used to recover black or white target pixels at the recipient.

B. Simple scrambling and unscrambling

Let's assume a set $\mathcal{X} = \{x_0, x_1, \dots, x_q, \dots, x_Q\}$ that is going to be scrambled in a simple way. In the approach, \mathcal{X} is separated into \mathcal{N} smaller sets, including $\frac{Q+1}{N}$ members, i.e. $\mathcal{N} \in \mathbb{N}$. In view on that, putting the corresponding members of each set together, scrambled one $\mathcal{Y} = \{y_0, y_1, \dots, y_i, \dots, y_Q\}$ is achieved. The number of members in \mathcal{X} set, $(Q+1)$, is selected in such a way divisible by \mathcal{N} . For example, regarding $\mathcal{X} = \{x_0, x_1, x_2, x_3, x_4, x_5\}$ and $\mathcal{N} = 3$, by dividing \mathcal{X} into 3 smaller sets, we have $\mathcal{X}_1 = \{x_0, x_1\}$, $\mathcal{X}_2 = \{x_2, x_3\}$ and $\mathcal{X}_3 = \{x_4, x_5\}$. The new positions, $\mathcal{Y} = \{x_0, x_2, x_4, x_1, x_3, x_5\}$, are achieved by putting the corresponding members of each set together.

Regarding simple scrambling, that scrambles \mathcal{X} to \mathcal{Y} , in a reverse procedure, \mathcal{Y} set is divided into $\frac{Q+1}{N}$ smaller ones including \mathcal{N} members and corresponding members of each set get together to reversibly bring out \mathcal{X} . As an example, considering $\mathcal{Y} = \{x_0, x_2, x_4, x_1, x_3, x_5\}$ and $\mathcal{N} = 3$, we divide \mathcal{Y} into 2 sets, $\mathcal{Y}_1 = \{x_0, x_2, x_4\}$ and $\mathcal{Y}_2 = \{x_1, x_3, x_5\}$. Putting together corresponding members of these two sets, $\mathcal{X} = \{x_0, x_1, x_2, x_3, x_4, x_5\}$ is retrieved outcome of a simple unscrambling.

C. MSB integration, disintegration and embedding data bits

In this section, we demonstrate procedure of embedding data bits in the integrated MSBs of the encrypted pixels. Employing integration, several MSBs must be changed instead of just one MSB to embed data bit that provides more resistant against failure of reconstruction.

This integration is done assigning a new binary level for \mathcal{N} -MSBs. It provides an integrated one less than $2^{\mathcal{N}}$. Using the histogram modification of the integrated MSBs some rooms are vacated to realize RDHEI.

Let's assume, $\hat{p}_q = \hat{p}_{(q,7)} \dots \hat{p}_{(q,3)} \dots \hat{p}_{(q,0)}$, as a bitwise demonstration of an encrypted pixel, i.e. from LSB, $\hat{p}_{(q,0)}$, to MSB, $\hat{p}_{(q,7)}$. As mentioned when (6) is confirmed for $p_q, \hat{p}_{(q,7)}$ may be replaced by a bit of data so that it would be perfectly retrievable. Having Q -MSBs of target pixels, $\hat{p}_7 = \{\hat{p}_{(0,7)}, \hat{p}_{(1,7)}, \dots, \hat{p}_{(q,7)}, \dots, \hat{p}_{(Q,7)}\}$, we describe process of

Algorithm 1: Shrinking the value of m_j for $(0 \leq j \leq \mathcal{J})$.

```

For  $j = 0$  to  $\mathcal{J}$  do
   $s_j = m_j$ 
  if  $(m_j < 2^{\mathcal{N}-1})$  then
     $s_j = 2^{\mathcal{N}} - 1 - m_j$ 
  end if
end for

```

Algorithm 2: Embedding data bits for $(1 \leq q < m \times l)$.

```

For  $j = 0$  to  $\mathcal{J}$  do
   $c_j = s_j$ 
  if  $(\hat{d}_q == 1)$  then
     $c_j = |2^{\mathcal{N}} - 1 - s_j|$ 
  end if
end for

```

integration by

$$m_j = \sum_{k=0}^{\mathcal{N}-1} 2^k \times (\hat{p}_{(q-k),7}), q = \mathcal{N} \times (j+1) - 1, j = 0, 1, \dots, \mathcal{J} \quad (8)$$

so integrated MSBs are denoted $\mathcal{M} = \{m_0, m_1, \dots, m_j, \dots, m_{\mathcal{J}}\}, 0 \leq m_j < 2^{\mathcal{N}}, \mathcal{J} = \frac{Q-N+1}{N}$.

Regarding the nature of the encrypted image, the histogram of \mathcal{M} demonstrates a uniform distribution. Embedding data bits in \mathcal{M} , we need to vacate rooms employing histogram modification of \mathcal{M} . The approach is a shrinking process that shifts each m_j less than $2^{\mathcal{N}-1}$ to a larger one. The shrunken ones, $\mathcal{S} = \{s_0, s_1, \dots, s_j, \dots, s_{\mathcal{J}}\}, 2^{\mathcal{N}-1} \leq s_j < 2^{\mathcal{N}}$, is achieved using Algorithm 1. In this algorithm, if $m_j < 2^{\mathcal{N}-1}$, it is reformed to s_j what has most bitwise mutation than m_j , i.e. m_j is replaced with its 1's complement.

Having rooms, $(\mathcal{J}+1)$ bits of the encrypted data, i.e. encrypted using K_d , $\hat{D} = \{\hat{d}_0, \hat{d}_1, \dots, \hat{d}_j, \dots, \hat{d}_{\mathcal{J}}\}$, may be embedded in \mathcal{S} employing Algorithm 2. In this algorithm, to embed an encrypted data bit with value "1" in s_j , it is replaced by its 1's complement and to embed value "0" it is remained intact.

Let's more precisely demonstrate the process of the embedding with an example having $\mathcal{N} = 3$ and integrated values of 27 MSBs, $\mathcal{M} = \{3, 0, 4, 7, 2, 2, 6, 1, 5\}$. Employing Algorithm 1, vacating rooms are done by shrinking procedure, $\mathcal{S} = \{4, 7, 4, 7, 5, 5, 6, 6, 5\}$. In other words, using histogram modification of \mathcal{M} , changing values between 0 and 3 to others, rooms are vacated to embed $\hat{D} = \{1, 1, 0, 1, 0, 0, 1, 0, 1\}$. Eventually, exploiting Algorithm 2 carrier set, $\mathcal{C} = \{3, 0, 4, 0, 5, 5, 1, 6, 2\}$, is achieved. Histogram of \mathcal{M} , \mathcal{S} and \mathcal{C} are depicted in Fig. 4-a, b and c respectively.

In order to create a marked encrypted image, at first, the set \mathcal{C} is disintegrated using

$$\left\lfloor \hat{p}_{((N \times j + k - 1),7)} \right\rfloor = \text{mod} \left(\left\lfloor \frac{c_j}{2^{\mathcal{N}-k}} \right\rfloor, 2 \right), 0 \leq j \leq \mathcal{J}, 0 < k \leq \mathcal{N} \quad (9)$$

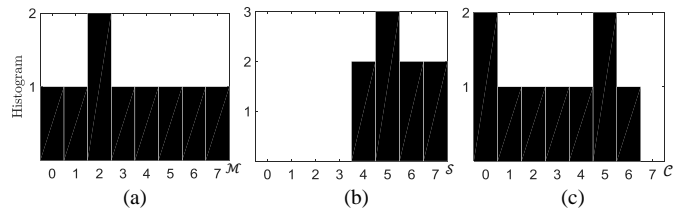


Fig. 4. The histogram of an example of \mathcal{M} , \mathcal{S} and \mathcal{C} sets.

Consequently, we have marked encrypted MSBs, $\{\hat{\mathcal{P}}_0, \hat{\mathcal{P}}_1, \dots, \hat{\mathcal{P}}_7, \dots, \hat{\mathcal{P}}_Q\}$. A marked pixel, $\hat{\mathcal{P}}_q$, $q = 0, 1, \dots, Q$, is created by replacement of a $\hat{\mathcal{P}}_{q,7}$ in MSB of $\hat{\mathcal{P}}_q$. Therefore, we have marked EWTPs, $\{\hat{\mathcal{P}}_0, \hat{\mathcal{P}}_1, \dots, \hat{\mathcal{P}}_q, \dots, \hat{\mathcal{P}}_Q\}$.

D. Extracting data bits

For extracting data bits, we just need data hider key, K_d . Firstly, MSBs of marked EWTPs as $\{\hat{\mathcal{P}}_7\}$ set are picked up and integrated to recover \mathcal{C} using (8) where $(\hat{\mathcal{P}}_{(q-k),7})$ and m_j respectively are replaced by $\hat{\mathcal{P}}_{(q-k),7}$ and c_j , $j = 0, 1, \dots, J$. In this paper, reconstructed sets or pixels are in bold.

Having $\mathcal{C} = \{c_0, c_1, \dots, c_j, \dots, c_J\}$, extracting data bits are done employing Algorithm 3. In Algorithm 3, j 'th bit of the encrypted data, $\hat{\mathcal{P}}_j$, is extracted using c_j . Encrypted bits are decrypted using k_d attaining \mathcal{D} .

E. Recovering the original image

Reconstructing the original image may be initiated by decryption of the marked encrypted image using K_e . Let's assume $\mathcal{P}' = \{\mathcal{P}'_0, \mathcal{P}'_1, \dots, \mathcal{P}'_q, \dots, \mathcal{P}'_Q\}$ is the decrypted white target pixels (DWTPs). The subject is reconstructing the MSBs of DWTPs, $\mathcal{P}'_7 = \{\mathcal{P}'_{0,7}, \mathcal{P}'_{1,7}, \dots, \mathcal{P}'_{q,7}, \dots, \mathcal{P}'_{Q,7}\}$. Other bits have been remained intact.

The reconstructing process continues by calculating 1's complement of \mathcal{P}'_7 that denoted $\mathcal{P}''_7 = \{\mathcal{P}''_{0,7}, \mathcal{P}''_{1,7}, \dots, \mathcal{P}''_{q,7}, \dots, \mathcal{P}''_{Q,7}\}$. By replacement of \mathcal{P}'_7 and \mathcal{P}''_7 in MSB of DWTPs we respectively have two different candidates of pixels $\mathcal{P}' = \{\mathcal{P}'_0, \mathcal{P}'_1, \dots, \mathcal{P}'_q, \dots, \mathcal{P}'_Q\}$ and $\mathcal{P}'' = \{\mathcal{P}''_0, \mathcal{P}''_1, \dots, \mathcal{P}''_q, \dots, \mathcal{P}''_Q\}$. Integrating \mathcal{N} -prediction-errors we have a cost function to choose a set of \mathcal{N} -pixels among these two candidate as recovered original set. In the following, we demonstrate this procedure in details.

After decryption, black pixels originally are recovered. They completely have been remained intact during embedding process and are employed to predict pixels of two candidates using (1) where \mathcal{P}_q is replaced by either \mathcal{P}'_q or \mathcal{P}''_q , $0 \leq q \leq Q$. Therefore, having predicted values of pixels for two different candidates, their prediction-errors $\mathcal{P}'_e = \{e'_0, e'_1, \dots, e'_q, \dots, e'_Q\}$ and $\mathcal{P}''_e = \{e''_0, e''_1, \dots, e''_q, \dots, e''_Q\}$ may be calculated using (2). In the following, integration of \mathcal{N} amounts of errors in \mathcal{P}'_e is achieved as an example for \mathcal{P}'_e by

$$\mathcal{E}'_j = \sum_{k=0}^{\mathcal{N}-1} |e'_{(q-k)}|, q = \mathcal{N} \times (j+1) - 1 \quad (10)$$

Similarly, \mathcal{E}''_j is attained by (10) for \mathcal{P}''_e where $e'_{(q-k)}$ is replaced with $e''_{(q-k)}$. Finally, the original \mathcal{N} -pixels belong to either \mathcal{P}' or \mathcal{P}'' are retrieved by comparing \mathcal{E}'_j and \mathcal{E}''_j employing Algorithm 4. Accordingly, for each j , if $\mathcal{E}''_j \leq \mathcal{E}'_j$ the recovered \mathcal{N} -pixels belong to \mathcal{P}'' and in vice versa they belong to \mathcal{P}' . Eventually, the recovered ones denote $\mathcal{P} = \{\mathcal{P}_0, \mathcal{P}_1, \dots, \mathcal{P}_q, \dots, \mathcal{P}_Q\}$.

Algorithm 3: Extracting data bits.

```

for  $j = 0$  to  $J$  do
  if  $(c_j < 2^{\mathcal{N}-1})$  then
     $d_j = 1$ 
  else if  $(2^{\mathcal{N}-1} \leq c_j < 2^{\mathcal{N}})$ 
     $d_j = 0$ 
  end if
end for

```

Algorithm 4: Reconstructing the original pixels.

```

for  $j = 0$  to  $J$  do
   $q = \mathcal{N} \times (j+1) - 1$ 
  if  $(\mathcal{E}''_j \leq \mathcal{E}'_j)$  then
     $[\mathcal{P}_{q-\mathcal{N}+1}, \dots, \mathcal{P}_q] = [\mathcal{P}''_{q-\mathcal{N}+1}, \dots, \mathcal{P}''_q]$ 
  else
     $[\mathcal{P}_{q-\mathcal{N}+1}, \dots, \mathcal{P}_q] = [\mathcal{P}'_{q-\mathcal{N}+1}, \dots, \mathcal{P}'_q]$ 
  end if
end for

```

Algorithm 5: Risk of LR.

```

if  $(\mathcal{R}_j < 16 \times \mathcal{N})$  then
  High risk (HiR)
else if  $(\mathcal{R}_j < 32 \times \mathcal{N})$  then
  Median risk (MeR)
else if  $(\mathcal{R}_j < 64 \times \mathcal{N})$  then
  Low risk (LoR)
else
  Very low risk (VLoR)
end if

```

Having $[\mathcal{P}_{q-\mathcal{N}+1}, \dots, \mathcal{P}_q] = [\mathcal{P}''_{q-\mathcal{N}+1}, \dots, \mathcal{P}''_q]$ means \mathcal{N} -pixels of the original image are losslessly reconstructed. If \mathcal{E}'_j and \mathcal{E}''_j are close together it will be a high risk in LR of the original pixels. Therefore, risk of LR may be analyzed by computing difference between \mathcal{E}'_j and \mathcal{E}''_j .

$$\mathcal{R}_j = |\mathcal{E}'_j - \mathcal{E}''_j| \quad (11)$$

The larger \mathcal{R}_j may be realized, the lower risk of LR can be attained and vice versa. Employing \mathcal{R}_j and \mathcal{N} in Algorithm 5, we can define 4 classes of risk: namely high risk (HiR), median risk (MeR), low risk (LoR) and very low risk (VLoR). Therefore, in each set of \mathcal{N} -pixels we have an analysis of risk. The bigger \mathcal{N} is chosen, the more accurate evaluation of risk is realized.

F. Overall view of the proposed method

In Fig. 5a, we depict general diagram of the proposed scheme. As shown, at first, embedding is done on EWTP as demonstrated in Subsection C. Then, in a similar way it can be

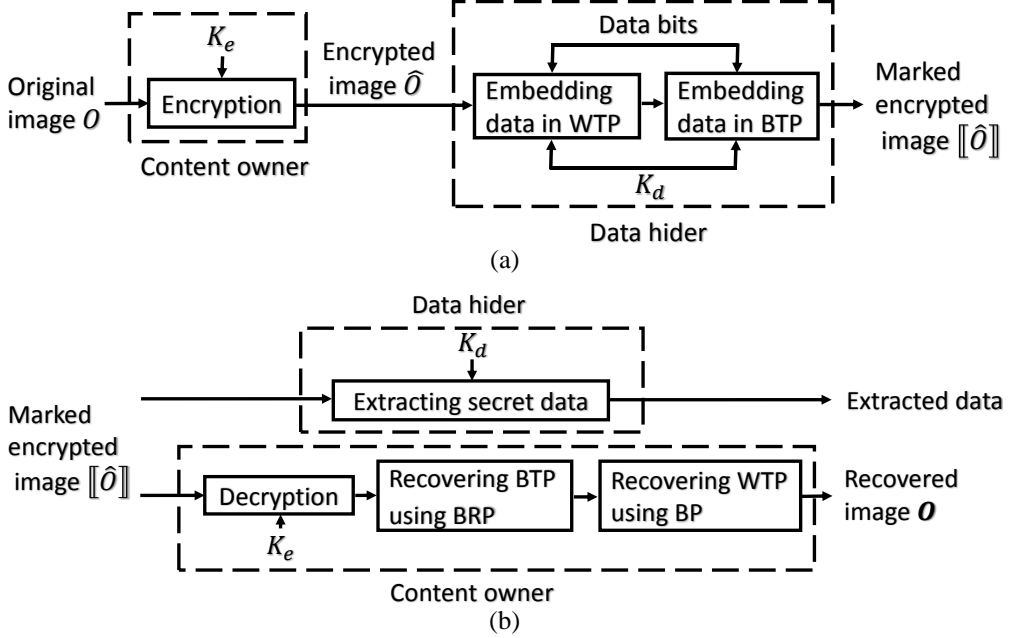


Fig. 5. Block diagram of the proposed scheme. (a) Embedding data and forming marked encrypted image. (b) Extracting data and recovering original image.

continued by EBTP, $\hat{P} = \{\hat{p}_0, \hat{p}_1, \dots, \hat{p}_q, \dots, \hat{p}_Q\}$ to increase EC. In more explanation, by choosing N -MSBs, integration can also be done for $\hat{P}_7 = \{\hat{p}_{0,7}, \hat{p}_{1,7}, \dots, \hat{p}_{q,7}, \dots, \hat{p}_{Q,7}\}$. N generally is considered bigger than N because, as discussed, WPP predictor can predict better than BCP one. Thus, integrated ones $M = \{m_0, m_1, \dots, m_j, \dots, m_J\}$, $0 \leq m_j < 2^N$, $J = \frac{Q-N+1}{N}$, are attained using (8) where m_j , p and N are replaced with m_j , p and N . Accordingly, marked EBTPs, $[\hat{P}] = \{[\hat{p}_0], [\hat{p}_1], \dots, [\hat{p}_q], \dots, [\hat{p}_Q]\}$, are achieved by doing all discussed steps in Subsection C, this time for \hat{P} . Eventually, marked encrypted image, including marked EWTPs and EBTPs, is created. Meanwhile, BRPs just are encrypted without any more modification. They will be employed to reconstruct other pixels at the recipient. They form 25% of the image.

Let's assume an original image in size $\mathbb{P} \times \mathbb{Q}$ so regarding a set of preferred $\{N, N\}$ and employing all target pixels including black and white, EC in bits is achieved by

$$EC = \mathbb{P} \times \mathbb{Q} \times \left(\frac{1}{2^N} + \frac{1}{4^N} \right) \quad (12)$$

so choosing $\{N = 1, N = 1\}$ most possible EC, $\frac{3}{4}(\mathbb{P} \times \mathbb{Q})$, is achieved.

In Fig. 5b, extracting data bits and reconstruction of the original image are described that can be done in a separable procedure.

Extracting data from marked EBTP, $[\hat{P}]$, similar to marked EWTP may be done as described in Subsection D.

Reconstructing the image is initiated by decryption of the marked encrypted image using K_c . Therefore, BRPs are completely recovered just by decryption. Using BRPs, BTPs may be recovered in a similar procedure described in Subsection E except using (3) and (4) instead of (1) and (2)

respectively to predict errors. Having black pixels, BPs, WTPs are recovered as also discussed in Subsection E. Risk of LR for N -pixels/ N -pixels can be computed in meanwhile of recovering.

The closer the pixels are the more correlation they have. By breaking the correlation, we can diminish risk of LR at the recipient. The approach may be realized by scrambling of MSB of target pixels before integration. In other words, the scrambling prevents integration of MSBs belong to near rough regions to keep together. Although, the scrambling can randomly be performed using K_d , for less complexity, in this scheme, we scramble the encrypted MSBs, \hat{P}_7/\hat{P}_7 , in a simple way (Subsection B). Thus, in more efficient procedure, the scrambled sets, are integrated, marked and finally unscrambled to form the corresponding marked encrypted pixels.

At the recipient, MSBs of encrypted target pixels are scrambled as well in the same approach for extracting data. Accordingly, at the recipient, for original image reconstruction, we must scramble prediction-errors. Therefore, in Algorithm 4, we should consider corresponding pixels of the scrambled prediction-errors for reconstructing original ones.

IV. EXPERIMENTAL RESULT

The performance of the proposed separable VRAE algorithm is confirmed designing several experiments. Twelve grayscale images F16, Lena, Splash, House, Boat, Elaine, Lake, Peppers, Baboon, Stream, Aerial and APC from the USC-SIPI database are used as test images. Also, BOWS2 original database, including 10000 greyscale images, are employed to confirm that the proposed algorithm can provide LR of the original image and error-free extraction of the data bits. All test

TABLE I PERFORMANCE ANALYSIS OF THE PROPOSED ALGORITHM EMPLOYING 12 TEST IMAGES.

Items	images											
	F16	Lena	Splash	House	Boat	Elaine	Lake	Peppers	Baboon	Stream	Aerial	APC
EC (bits)	161290	161290	161290	161290	86021	193548	96774	161290	86021	80645	86021	96774
\mathcal{N}	1	1	1	1	2	1	2	1	2	2	2	2
N	2	2	2	2	3	1	2	2	3	4	3	2
PSNR	∞											
\mathcal{N} -pixels	HiR	4	0	0	0	0	0	8	5	0	0	0
sets	MeR	136	80	4	163	44	27	2	161	1052	182	130
N -pixels	HiR	0	0	0	0	0	1	0	0	13	0	0
sets	MeR	37	9	1	33	68	40	93	35	885	25	103

images are 512×512 in size. In experiments, the first and the last two rows and columns of the image are ignored in data embedding process. Peak signal-to-noise ratio (PSNR) is used to estimate the quality of a recovered image. $\text{PSNR} = \infty$ means LR of the original image.

Choosing a set of $\{\mathcal{N}, N\}$ may be tied to entropy of an image. The greater the entropy of the image is estimated, the greater the value of $\{\mathcal{N}, N\}$ must be selected for LR. However, the more $\{\mathcal{N}, N\}$ is preferred, the less EC is attained. Therefore, there is a tradeoff between EC and PSNR of the reconstructed image. In Table I, the precise \mathcal{N}/N for LR of the test images is inserted. By taking $\{\mathcal{N} = 1, N = 1\}$ for Elaine the most possible EC in the proposed method, 193548 bits, is achieved. In the other side, Stream image provides lowest EC. In this image, the lowest possible \mathcal{N}/N for LR is $\{\mathcal{N} = 2, N = 4\}$ that definitely may be employed for LR of the other test images. Also, in the table, risk of LR is evaluated by computing the number of \mathcal{N} -pixels that take HiR or MeR. Although F16, Peppers and Baboon are reconstructed perfectly, respectively include 4, 8 and 5 high risk sets of \mathcal{N} -pixels. Also, in reconstructing the sets of N -pixels, Baboon and Elaine take 13 and 1 sets of high risk, respectively. Accounting the number of HiR and MeR sets, generally, Baboon have most risk of LR. However, by choosing $\{\mathcal{N} = 3, N = 5\}$ for embedding data in Baboon, no set of HiR is left. It is attained by paying the cost of diminishing EC to 55913 bits.

On the other hand, we assume that data hider in the proposed scheme is completely blind to the original-content so we can not find out the least possible precise $\{\mathcal{N}, N\}$ for LR. However, in the next subsection we confirm that a set of $\{\mathcal{N}, N\}$ may be

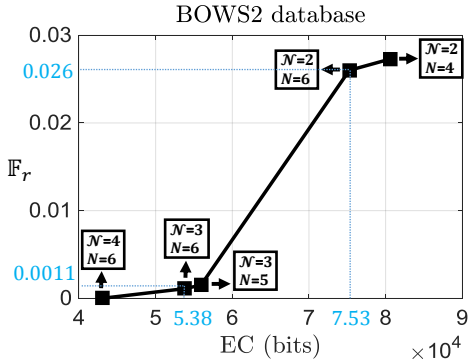


Fig. 6. Efficiency evaluation of the proposed algorithm employing 10000 test images of Bows2 database in different sets of $\{\mathcal{N}, N\}$. We just exploit K_e to restore original images. F_r is failure rate.

always found out for LR.

In the proposed scheme, error-free extraction of data bits is realized for all test images under any circumstances.

A. Lossless retrieval

In Fig. 6 we demonstrate performance of the proposed scheme in LR and error-free extraction of data bits using 10000 test images of BOWS2 original database. As shown, for various $\{\mathcal{N}, N\}$ we accomplished the proposed algorithm to bring out the number of failure in LR. For example, in $\{\mathcal{N} = 3, N = 6\}$, from 10000 test images there is 11 images that are not perfectly reconstructed so the failure rate is $F_r = 0.0011$. As shown, the more $\{\mathcal{N}, N\}$ is preferred, the less EC and obviously the less failure rate are provided. In $\{\mathcal{N} = 4, N = 6\}$, F_r is zero. Thus, there exists permanently a set of $\{\mathcal{N}, N\}$ to provide LR for all 10000 test images.

As shown in the figure, modifying \mathcal{N} affects EC and F_r more than N . As instance, in $N = 6$, increasing \mathcal{N} from 2 to 3 diminishes EC and F_r as much as 21506 bits and 0.0249, respectively while in $\mathcal{N} = 3$, increment of N has no noticeable impact on EC and F_r .

Implementing the proposed algorithm by $\{\mathcal{N} = 3, N = 6\}$, we descendingly sort all 10000 reconstructed images by the number of their \mathcal{N} -pixels that are HiR. As discussed, in this implementation, all failures are 11. The first six sorted images are listed in Table II. In the table, PSNR demonstrates four images that is not reconstructed losslessly and so 4 out of all 11 failures include in first six sorted images. It proves risk analysis is a proper assessment for evaluation LR, i.e. all 11 failures are included in 50 first sorted images. In any failure, there exist some deformed MSBs that can not be recovered correctly. The number of deformed MSBs are demonstrated in Table II for images. The maximum one is just 12 bits for 6501.pgm image so there is not much error rate of bits when LR does not realized.

B. A visual demonstration of the proposed scheme

Fig. 7 is a visual demonstration of the proposed procedure including original, encrypted, marked encrypted and reconstructed images with their depicted histograms. We optionally employ AES in counter mode, i.e. a stream cipher procedure, to encrypt Lena test image. As shown in Fig. 7b, after encryption there exist no knowledge of the original image remaining discovered. As a proof, its histogram is uniformly distributed. We guarantee the security of the proposed

algorithm because of having two important property: 1- There is no feature or knowledge of the original-content that remains disclosed. 2- Choosing a desire encryption algorithm is possible regarding its pros and cons including the security. Since in the proposed method, data hider is completely blind to the original-content, it absolutely preserves content-owner privacy. Moreover, content owner can encrypt original-content using any key-based encryption algorithm including stream or block cipher.

Fig. 7c is a description of the marked encrypted image. The histogram still has a uniform distribution. Original image is losslessly reconstructed as shown in Fig. 7d.

C. Comparison with other schemes

Separable VRAE methods are more functional than others. The proposed scheme is an only one of separable VRAE methods that makes possible LR of the original image just by having secret key (K_e). There exist some experiments to confirm it.

In Table III, proposed scheme is compared with other separable VRAE schemes. Schemes [27] and [29] compress some bits of encrypted pixels to vacate room in order to embed data bits. Meanwhile, they employ some parameters can be used to form a tradeoff between EC and lossless recovery. Their functionality is similar to \mathcal{N}/N . For fairness comparison between our method and [27] and [29] we employ these parameters so that LR of the all test images is accomplished. In the approach, we apply parameters $\{M = 4, S = 2, L = 271\}$, $\{q = 0.1\}$ and $\{\mathcal{N} = 2, N = 3\}$ to [27], [29], and ours, respectively. It should be noted that by choosing less L, q and \mathcal{N} , both EC and risk of LR are enlarged respectively in [27], [29] and ours. It generally leads more probability of failure in LR.

In [29], for LR at the recipient, some information is needed that can be available just by employing K_d . Therefore, as demonstrated in Table III, for this scheme just a high quality version of the original image can be retrieved without having K_d while in the proposed scheme LR of the original image can be accomplished. Besides, our algorithm can achieve more EC than [29].

As described in Table III, in comparison with [27] we significantly improve EC. Similar to [29] their algorithm is dependent to having K_d for LR of the original image.

In [32] scheme, using data hider key, they prefer some target pixels in the encrypted image to embed data bits and employ a predictor may be denoted a modified WPP predictor to reconstruct original image at the recipient. Their methods do not guarantee LR, although it may be possible by diminishing the number of selected target pixels. In this experiment, we consider the most number of target pixels may be chosen in [32] scheme. In the approach, their algorithm fails in perfect reconstruction of the original image for five test images. As described in Table III, we improve their algorithm designing a procedure to guarantee LR by employing histogram modification and MSBs integration. However, we pay the cost by less EC. All discussed schemes and ours provide an error-free data bits extraction

In Fig. 8 we compare our scheme with [16], [27], [29], [30] and [32] in quality of the reconstructed original image. In this experiment for reconstructing we suppose schemes [30] and [32] have both encryption and data hider keys while others just have encryption key. In [30] method, original image reconstruction and data bits extraction are joint while our scheme is a separable one. In comparison, we improve not only EC but also image quality. To embed data bits, scheme [16] reserves rooms before encryption aim of patch-level sparse representation. Generally, achieving EC in the proposed scheme is comparable with this scheme. In their work, a preprocessing is allowed before encryption while we absolutely are blind to original-content.

As shown in Fig. 8, scheme [29] outperforms schemes [16] and [27] in term of PSNR. Achieving LR, we outperform scheme [29].

In comparison with scheme [32], for Peppers and Lena we improve EC. In Lake, Peppers and Baboon they achieve a PSNR less than 55 dB even by using both keys while we realize LR just by K_e .

V. CONCLUSION

In this paper, by comparing different predictors, we show that WPP is the better one used to diminish probability of failure in reconstruction of the original image. Moreover, BCP predictor is employed to increase embedding capacity. By prediction-error analysis, we just choose MSB of encrypted target pixels to embed data bits. These MSBs are integrated to be more resistant against failure of reconstruction when they are modified to embed data bits. Employing histogram modification of the integrated ones, we vacate rooms to embed data bits. At the recipient, in a separable way data bits are extracted and original image is reconstructed. We employ the risk analysis to have a probability of LR.

TABLE II SIX IMAGES OF BOWS2 ORIGINAL DATABASE THAT HAVE MOST THE NUMBER OF HiR SETS OF \mathcal{N} -PIXELS.

Items	Images (.pgm)					
	6502	6501	6537	6498	6514	9373
\mathcal{N} -pixels sets	HiR	15	11	10	6	4
	MeR	947	923	778	943	415
N -pixels sets	HiR	1	1	2	1	0
	MeR	285	259	413	415	60
PSNR		52.39	49.38	∞	52.39	55.4
The number of deformed-MSBs		6	12	0	6	0

TABLE III EFFICIENCY COMPARISON BETWEEN THE PROPOSED METHOD AND OTHER SEPARABLE VRAE ONES FOR 9 TEST IMAGES.

Schemes	Items	images								
		F16	Lena	Splash	House	Boat	Elaine	Lake	Peppers	Baboon
Zhang2012 [27]	EC (bits)	1920	1920	1920	1920	1920	1920	1920	1920	1920
	LR	Pass								
	LR just by K_e	Fail								
Wu [32]	EC (bits)	130050								
	LR	Pass	Pass	Pass	Fail	Fail	Pass	Fail	Fail	Fail
	LR just by K_e	Pass	Pass	Pass	Fail	Fail	Pass	Fail	Fail	Fail
Qian [29]	EC (bits)	77376	77376	77376	77376	77376	77376	77376	77376	77376
	LR	Pass								
	LR just by K_e	Fail								
Proposed scheme	EC (bits)	86021								
	LR	Pass								
	LR just by K_e	Pass								

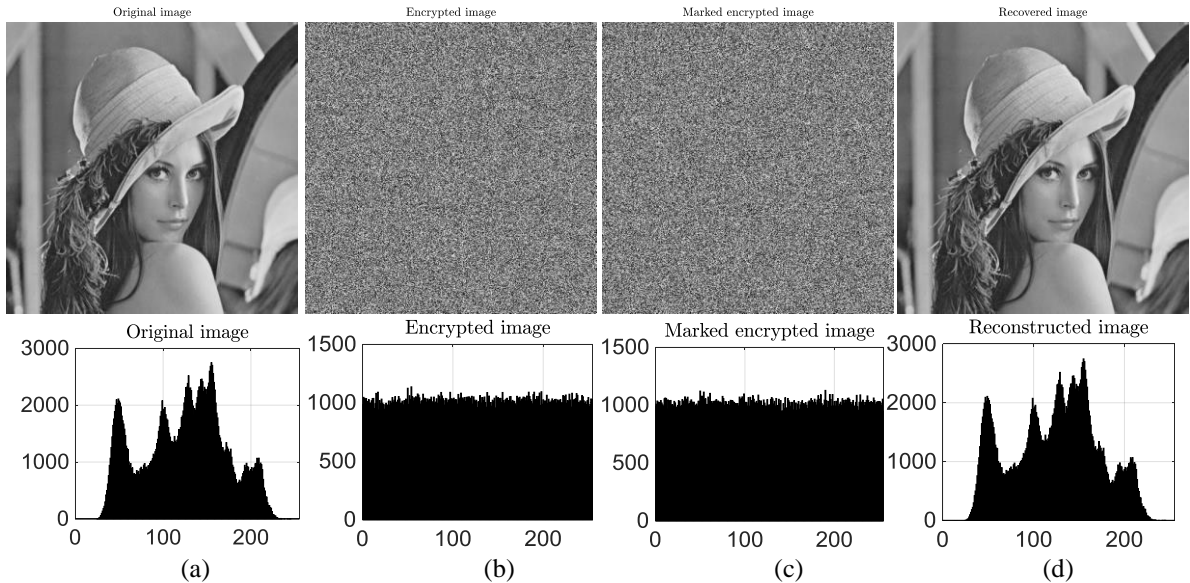


Fig. 7. A visual demonstration of the proposed scheme.

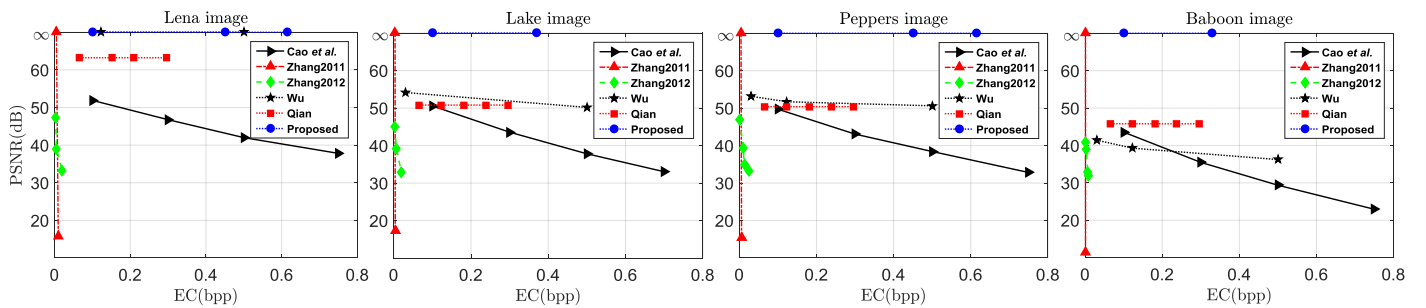


Fig. 8. PSNR comparison between our proposed scheme and other schemes Cao et al. [16], Zhang2011 [30], Zhang2012 [27], Qian [29] and Wu [32] for four test images.

The proposed method improves other separable VRAE schemes by aim of MSBs integration and histogram modification. We are the only one that realizes LR without having K_d .

REFERENCES

- [1] Y.-Q. Shi, X. Li, X. Zhang, H.-T. Wu, and B. Ma, "Reversible data hiding: advances in the past two decades," *IEEE Access*, vol. 4, pp. 3210-3237, 2016.
- [2] J. Tian, "Reversible data embedding using a difference expansion," *IEEE Transactions on Circuits and Systems for Video Technology*, vol. 13, no. 8, pp. 890-896, Aug. 2003.
- [3] Z. Ni, Y.-Q. Shi, N. Ansari, and W. Su, "Reversible data hiding," *IEEE Transactions on Circuits and Systems for Video Technology*, vol. 16, no. 3, pp. 354-362, Mar. 2006.
- [4] T. Kalker, and F. M. Willems, "Capacity bounds and constructions for reversible data-hiding," in *Proc. International Conference on Digital Signal Processing*, Santorini, Greece, 2002, pp. 71-76.
- [5] X. Li, W. Zhang, X. Gui, and B. Yang, "A novel reversible data hiding scheme based on two-dimensional difference-histogram modification," *IEEE Transactions on Information Forensics and Security*, vol. 8, no. 7, pp. 1091-1100, Jul. 2013.
- [6] D. M. Thodi, and J. J. Rodríguez, "Expansion embedding techniques for reversible watermarking," *IEEE Transactions on Image Processing*, vol. 16, no. 3, pp. 721-730, Mar. 2007.
- [7] X. Wu, and N. Memon, "Context-based, adaptive, lossless image coding," *IEEE Transactions on Communications*, vol. 45, no. 4, pp. 437 - 444, Apr. 1997.
- [8] M. J. Weinberger, G. Seroussi, and G. Sapiro, "The LOCO-I lossless image compression algorithm: Principles and standardization into JPEG-LS," *IEEE Transactions on Image processing*, vol. 9, no. 8, pp. 1309-1324, Aug. 2000.
- [9] P. Tsai, Y.-C. Hu, and H.-L. Yeh, "Reversible image hiding scheme using predictive coding and histogram shifting," *Signal Processing*, vol. 89, no. 6, pp. 1129-1143, Jun. 2009.
- [10] V. Sachnev, H. J. Kim, J. Nam, S. Suresh, and Y. Q. Shi, "Reversible watermarking algorithm using sorting and prediction," *IEEE Transactions on Circuits and Systems for Video Technology*, vol. 19, no. 7, pp. 989-999, Jul. 2009.
- [11] A. Mohammadi, and M. Nakhkash, "Sorting methods and adaptive thresholding for histogram based reversible data hiding," *arXiv preprint arXiv:1907.05129*, 2019.
- [12] S. Xiang, and X. Luo, "Reversible data hiding in homomorphic encrypted domain by mirroring ciphertext group," *IEEE Transactions on Circuits and Systems for Video Technology*, vol. 28, no. 11, pp. 3099-3110, Nov. 2018.
- [13] K. Ma, W. Zhang, X. Zhao, N. Yu, and F. Li, "Reversible data hiding in encrypted images by reserving room before encryption," *IEEE Transactions on Information Forensics and Security*, vol. 8, no. 3, pp. 553-562, Mar. 2013.
- [14] Z. Yin, Y. Xiang, and X. Zhang, "Reversible data hiding in encrypted images based on multi-MSB prediction and huffman coding," *IEEE Transactions on Multimedia*, Aug. 2019.
- [15] Y.-C. Chen, T.-H. Hung, S.-H. Hsieh, and C.-W. Shiu, "A new reversible data hiding in encrypted image based on multi-secret sharing and lightweight cryptographic algorithms," *IEEE Transactions on Information Forensics and Security*, vol. 14, no. 12, pp. 3332-3343, Dec. 2019.
- [16] X. Cao, L. Du, X. Wei, D. Meng, and X. Guo, "High capacity reversible data hiding in encrypted images by patch-level sparse representation," *IEEE Transactions on Cybernetics*, vol. 46, no. 5, pp. 1132-1143, May, May 2016.
- [17] C.-W. Shiu, Y.-C. Chen, and W. Hong, "Encrypted image-based reversible data hiding with public key cryptography from difference expansion," *Signal Processing: Image Communication*, vol. 39, pp. 226-233, Nov. 2015.
- [18] P. Pueaux, and W. Puech, "An efficient MSB prediction-based method for high-capacity reversible data hiding in encrypted images," *IEEE Transactions on Information Forensics and Security*, vol. 13, no. 7, pp. 1670-1681, Jul. 2018.
- [19] A. Mohammadi, and M. Nakhkash, "Reversible data hiding in encrypted images using local difference of neighboring pixels," *arXiv preprint arXiv:1907.05123*, 2019.
- [20] S. Yi, and Y. Zhou, "Separable and reversible data hiding in encrypted images using parametric binary tree labeling," *IEEE Transactions on Multimedia*, vol. 21, no. 1, pp. 51-64, Jan. 2019.
- [21] D. Xu, and R. Wang, "Separable and error-free reversible data hiding in encrypted images," *Signal Processing*, vol. 123, pp. 9-21, Jun. 2016.
- [22] Z. Yin, B. Luo, and W. Hong, "Separable and error-free reversible data hiding in encrypted image with high payload," *The Scientific World Journal*, vol. 2014, Apr. 2014.
- [23] W. Zhang, K. Ma, and N. Yu, "Reversibility improved data hiding in encrypted images," *Signal Processing*, vol. 94, no. 1, pp. 118-127, Jan. 2014.
- [24] F. Huang, J. Huang, and Y.-Q. Shi, "New framework for reversible data hiding in encrypted domain," *IEEE Transactions on Information Forensics and Security*, vol. 11, no. 12, pp. 2777-2789, Dec. 2016.
- [25] H. Ge, Y. Chen, Z. Qian, and J. Wang, "A high capacity multi-level approach for reversible data hiding in encrypted images," *IEEE Transactions on Circuits and Systems for Video Technology*, vol. 29, no. 8, pp. 2285 - 2295, Aug. 2019.
- [26] X. Zhang, "Commutative reversible data hiding and encryption," *Security and Communication Networks*, vol. 6, no. 11, pp. 1396-1403, 2013.
- [27] X. Zhang, "Separable reversible data hiding in encrypted image," *IEEE Transactions on Information Forensics and Security*, vol. 7, no. 2, pp. 826-832, Apr. 2012.
- [28] J. Zhou, W. Sun, L. Dong, X. Liu, O. C. Au, and Y. Y. Tang, "Secure reversible image data hiding over encrypted domain via key modulation," *IEEE Transactions on Circuits and Systems for Video Technology*, vol. 26, no. 3, pp. 441-452, Mar. 2016.
- [29] Z. Qian, and X. Zhang, "Reversible data hiding in encrypted images with distributed source encoding," *IEEE Transactions on Circuits and Systems for Video Technology*, vol. 26, no. 4, pp. 636-646, Apr. 2016.
- [30] X. Zhang, "Reversible data hiding in encrypted image," *IEEE Signal Processing Letters*, vol. 18, no. 4, pp. 255-258, Apr. 2011.
- [31] W. Hong, T.-S. Chen, and H.-Y. Wu, "An improved reversible data hiding in encrypted images using side match," *IEEE Signal Processing Letters*, vol. 19, no. 4, pp. 199-202, Apr. 2012.
- [32] X. Wu, and W. Sun, "High-capacity reversible data hiding in encrypted images by prediction error," *Signal Processing*, vol. 104, pp. 387-400, Nov. 2014.
- [33] M. Fallahpour, and M. H. Sedaaghi, "High capacity lossless data hiding based on histogram modification," *IEICE Electronics Express*, vol. 4, no. 7, pp. 205-210, 2007.